

An Efficient Hybrid DSMC/MD Algorithm for Accurate Modeling of Micro Gas Flows

Tengfei Liang¹ and Wenjing Ye^{1,2,*}

¹ Department of Mechanical Engineering, Hong Kong University of Science and Technology, Clear Water Bay, Kowloon, Hong Kong.

² KAUST-HKUST Micro/Nanofluidic Joint Laboratory, Hong Kong University of Science and Technology, Clear Water Bay, Kowloon, Hong Kong.

Received 14 November 2012; Accepted (in revised version) 16 May 2013

Available online 15 August 2013

Abstract. Aiming at simulating micro gas flows with accurate boundary conditions, an efficient hybrid algorithm is developed by combining the molecular dynamics (MD) method with the direct simulation Monte Carlo (DSMC) method. The efficiency comes from the fact that the MD method is applied only within the gas-wall interaction layer, characterized by the cut-off distance of the gas-solid interaction potential, to resolve accurately the gas-wall interaction process, while the DSMC method is employed in the remaining portion of the flow field to efficiently simulate rarefied gas transport outside the gas-wall interaction layer. A unique feature about the present scheme is that the coupling between the two methods is realized by matching the molecular velocity distribution function at the DSMC/MD interface, hence there is no need for one-to-one mapping between a MD gas molecule and a DSMC simulation particle. Further improvement in efficiency is achieved by taking advantage of gas rarefaction inside the gas-wall interaction layer and by employing the "smart-wall model" proposed by Barisik *et al.* The developed hybrid algorithm is validated on two classical benchmarks namely 1-D Fourier thermal problem and Couette shear flow problem. Both the accuracy and efficiency of the hybrid algorithm are discussed. As an application, the hybrid algorithm is employed to simulate thermal transpiration coefficient in the free-molecule regime for a system with atomically smooth surface. Result is utilized to validate the coefficients calculated from the pure DSMC simulation with Maxwell and Cercignani-Lampis gas-wall interaction models.

PACS: 47.45.-n, 34.35.+a, 47.11.St, 47.61.-k

Key words: Rarefied gas flows, surface effect, multi-scale methods.

*Corresponding author. *Email addresses:* tfliang@ust.hk (T. Liang), mewye@ust.hk (W. Ye)

1 Introduction

Gas flows are frequently encountered and utilized in microelectromechanical (MEMS) systems, for example, the pressure gas flows in micro channels and flows surrounding micro resonators and the heated micro plate in Pirani sensors. Gas transport and its interaction with the devices play important roles in device operation and accurate modeling of gas flows is crucial to the design of high-performance MEMS devices [1]. One distinct feature of micro gas flows is the rarefaction caused by the small characteristic size and/or the low ambient pressure. In addition, the large surface-to-volume ratio of MEMS devices dictates a surface-dominant transport. As is well known, Navier-Stokes equations and the no-slip boundary model become increasingly inaccurate as the rarefaction level increases. Alternative approaches are therefore adopted for the modeling of rarefied gas.

There have been numerous approaches developed for the modeling of micro gas flows. Examples include but are not limited to the direct simulation of Boltzmann equation [2–4], kinetic schemes [5, 6], physical simulation methods such as molecular dynamics (MD) [7] and the direct simulation Monte Carlo (DSMC) [8]. A common key ingredient in all these approaches is a proper boundary model describing correctly the gas-wall interaction process. Other than the MD approach, almost all other methods employ a phenomenological model built upon statistically averaged particle flux distribution. Currently the two most popular models are Maxwell model [9] and Cercignani-Lampis (CL) model [10]. Despite numerous successful applications of these models particularly in the modeling of high-speed rarefied gas transport, the empirical nature and the need of several parameters denoted as the accommodation coefficients demand a careful assessment of the models and a method to determine the accommodation coefficients for applications related to micro gas flows that are often of low speed. Considerate efforts have been made to experimentally measure the accommodation coefficients in MEMS devices [11, 12]. The challenges encountered such as leakage and being prone to temperature variation make it difficult to conduct accurate measurement, which is reflected in part by the discrepancies among the reported values in the literature [13].

The MD method, by tracking the motion of individual molecule, is able to model gas-wall interaction accurately, and has been employed in some cases to validate the empirical models and obtain accommodation coefficients [14–16]. It has been shown that gas-wall scattering process cannot be fully captured by the empirical gas-wall interaction models particularly when the incident gas molecules are at a highly non-equilibrium state [14, 16]. A major deficiency of the MD method is its high computational cost. For most micro flow problems, it is impractical to apply the MD method to simulate the entire flow domain. A natural choice is to couple the MD method with other more efficient approaches so that the computationally expensive MD method is applied only in the region where it is needed. The DSMC method is an excellent candidate to be coupled with the MD method. Both approaches are particle based so that the coupling between the two methods is relatively easy to realize. The DSMC, although still computational intensive, is much more efficient than the MD for diluted gas and it has been demonstrated in

numerous examples that it is possible to apply the DSMC method for the modeling of realistic MEMS flow problems [17–19].

Although limited, there has been some work on the development of hybrid MD/DSMC schemes, for example, those described in [15,20,21]. An excellent review of some of the work can be found in [21]. In all these approaches, the MD is applied in the gas region next to either a solid wall or a liquid interface, while the DSMC is applied in the rest of the gas domain. The main difference between different schemes is the coupling strategy. To maintain the continuity of mass, momentum and heat flux at the interface of the two simulation domains in any hybrid algorithm is not trivial. The scheme developed by Gu, *et al.* [21] uses one real gas molecule as the simulation particle in the DSMC simulation, and hence the coupling between the two domains is simply conducted by passing one DSMC simulation particle directly into one MD molecule and vice versa. The downside of the scheme is the compromised efficiency in the DSMC simulation. In addition, the inherent noise in the DSMC quantities, if is not reduced before being passed into the MD region, may cause problems. In most multiscale simulations, MD simulation often dominates the total computational cost. Hence the reduction of MD portion of the simulation would be very effective to further improve the overall efficiency. Barisik *et al.* [22,23] proposed a virtually movable “smart wall” model to represent the entire rigid wall boundary in MD simulation, which greatly reduced the memory requirement in the simulation of the rigid wall.

The previously developed schemes target at the problems in which accurate molecular transport within the gas-wall interaction layer (GWIL) characterized by the cut-off distance of the interaction potential is important. In many practical problems, the field of interest is the flow region outside the thin GWIL. To obtain accurate macroscopic quantities in this region, the detailed molecular information within the GWIL is not necessary provided that the velocity distribution function of the reflected molecules can be obtained. This in fact is the foundation on which methods such as the DSMC, kinetic schemes and direct simulation of Boltzmann equation based. In this paper, a new scheme in which the MD method is employed primarily for obtaining accurate velocity distribution function of the reflected molecules is introduced. The goal is to obtain accurate boundary conditions for the DSMC or other methods based on velocity distribution function.

In the following section, a description of the new hybrid algorithm is provided, followed by the validation of the developed algorithm on two benchmarks, namely Fourier thermal problem and Couette shear flow problem. The application of the hybrid scheme in the modeling of thermal transpiration problem is described next. Lastly a brief summary of the work is presented to conclude the paper.

2 Description of the hybrid algorithm

As mentioned in the introduction, the objective of the new hybrid scheme is to provide accurate solutions of gas transport outside the gas-wall interaction layer. Such an objec-

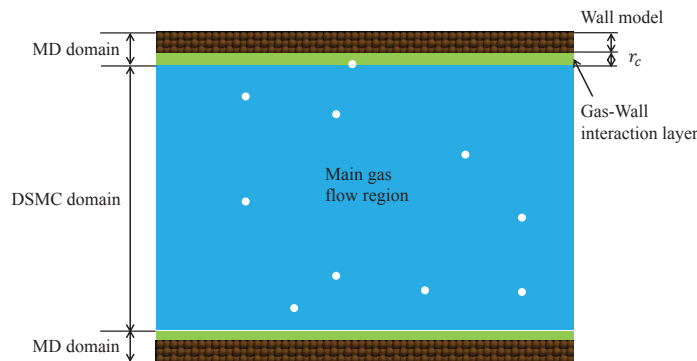


Figure 1: A schematic illustration of the domain partition.

tive can be realized by using the DSMC together with the accurate velocity distribution function of reflected gas molecules provided by MD simulation. Fig. 1 illustrates the partition of the simulation domain in which the MD region includes the gas-wall interaction layer and the solid wall, and the DSMC domain covers the remaining portion of the gas domain. The thickness of the gas-wall interaction layer is determined by the cut-off distance of the gas-solid interaction potential. Hence molecules inside the DSMC region do not experience any force directly from the solid wall.

As in any hybrid scheme, the coupling between different simulation methods/ domains is the most crucial step. Unlike some previous hybrid schemes in which the coupling between the MD and the DSMC domain is particle based, for example, in the scheme of Gu *et al.* [21] one DSMC simulation particle is directly mapped into one MD molecule, the coupling of the present scheme is through velocity distribution function at the DSMC/MD interface. DSMC simulation provides the velocity distribution function of gas molecules entering the MD domain from which MD gas molecules are generated, in the meantime those molecules entering the DSMC domain are generated based on the reflected velocity distribution function simulated from MD simulation. There is no one-to-one correspondence between the MD molecules and DSMC particles. Hence the efficiency of the DSMC simulation retains since one simulation particle can still represent a large cluster of real molecules. In addition, the conservation requirements of mass, momentum and energy are satisfied across the interface of the two domains naturally due to the matching of the velocity distribution function.

The main steps of the scheme are illustrated in Fig. 2. Simulation starts with the initialization step in which simulation particles in the DSMC domain and gas molecules in the MD domain are generated based on the initial conditions. Next, both MD and DSMC simulations are advanced for one updating time step. During this time step, molecules/simulation particles crossing the interface from either domain are recorded and discarded from the respective domain. The velocities of these particles/molecules are used to obtain the discretized velocity distributions. This is achieved by discretizing the velocity space into many small intervals and counting the probability density of each

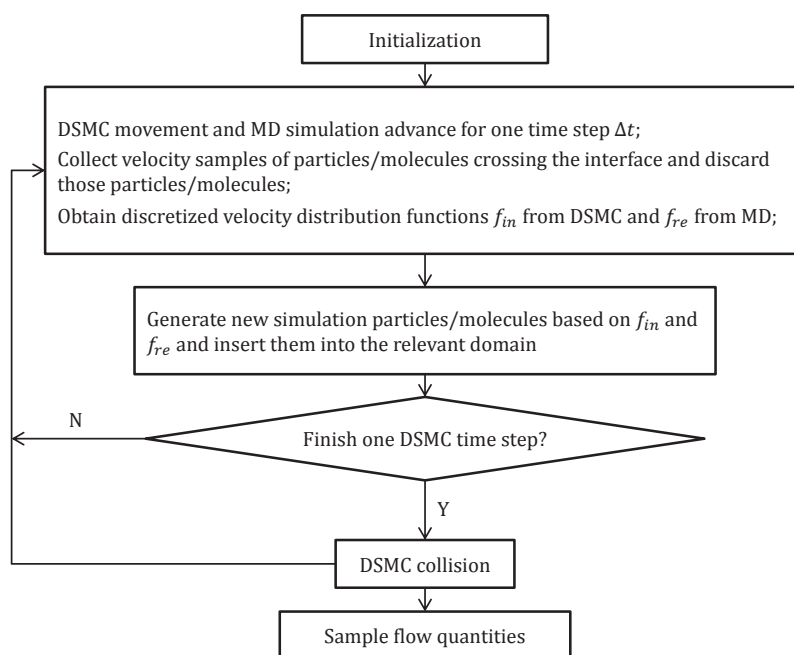


Figure 2: The flow chart of the hybrid scheme.

interval based on the velocity samples. To obtain enough samples, an ensemble of different realizations of the system should be simulated concurrently for unsteady problems. For steady problems, such a process can be replaced by a time averaging approach. Based on these distribution functions, new MD molecules and DSMC simulation particles are generated and inserted into the respective domain at the end of this updating time step. This procedure repeats until the accumulated computational time reaches to one DSMC time step. Then DSMC collision takes place and simulation returns back to step 2, that is, the step after initialization, and continues until finish. The updating time step determines how often the two domains are communicated. The upper and lower bounds for this time step are the DSMC and MD time steps respectively. In general, the smaller the step is, the more accurate the results are. However the associated computational time also increases. In this study, the updating time step Δt is set to be one DSMC time step.

It is clear that the computational time of the scheme is dominated by the MD simulation. To reduce the time as well as the memory consumption, the "smart wall" model proposed by Barisik *et al.* [22] can be employed which significantly reduces the number of solid wall molecules. In order to simulate thermal wall, the original smart-wall algorithm initially designed for rigid walls has been modified. Instead of using 74 solid atoms to form a hemisphere rigid wall lattice, the new wall stencil used in this work is a cuboid wall element formed by 400 solid atoms ($10 \times 10 \times 4$), which satisfies the "minimum image convention". Solid atoms are connected through the solid-solid interaction potential. Periodical boundary conditions are applied in the lateral directions of the wall

stencil. Impinging gas molecules are assigned into the corresponding wall stencil based on their locations and gas-wall interaction is simulated within each wall stencil coupled with the periodic boundary conditions for the wall stencil. Furthermore, for cases when gas is highly rarefied inside the gas-wall interaction layer, the gas-gas interaction inside this layer can be neglected without compromising the accuracy of the velocity distribution function of the reflected gas molecules. With this simplification, not only the time spent on the calculation of gas-gas interaction is saved, but also the gas-wall interaction can be simulated in parallel, leading to a much more efficient MD algorithm.

The error introduced by neglecting gas-gas interaction inside the gas-wall interaction layer can be estimated based on the ratio of two time scales, the mean residence time $\bar{\tau}$, that is, the time gas molecules stay inside the interaction layer, and the mean gas-gas molecular collision interval in the GWIL τ_c . If $\bar{\tau}/\tau_c < 1$, which is roughly equivalent to having a local Knudsen number (Kn) larger than 1 in the gas-wall interaction layer, the interaction between gas molecules might be negligible there. The mean residence time $\bar{\tau}$ can be obtained from the MD simulation of the gas-wall scattering process. The calculation of τ_c needs the gas density, n_{GWIL} , inside the GWIL, which can be estimated based on the balance between the inward and outward number flux of gas molecules at the DSMC/MD interface, as shown in Eq. (2.1),

$$\frac{1}{4}n_0\bar{C} = \frac{n_{GWIL}h}{\bar{\tau}}. \quad (2.1)$$

The left-hand side of the equation describes the incident number flux, where n_0 and \bar{C} are the number density and mean molecular velocity of the incident molecules. The right-hand side of the equation is the average number flux of gas molecules flowing out of the GWIL, where h is the effective thickness of the GWIL determined based on the potential between a gas molecule and the entire solid wall, it is slightly smaller than the nominal thickness of the GWIL determined by the cut-off distance of the interaction potential between a gas molecule and a solid atom. Gas densities n_{GWIL} near the two walls in the 1-D Fourier thermal problem of Section 3.1 are estimated from Eq. (2.1) and results agree well with that simulated from pure MD simulation.

The time ratios $\bar{\tau}/\tau_c$ of three typical systems, namely Ar-Pt, Ar-Si and N₂-Pt, at the room temperature 300K and 1 atm are calculated and listed in Table 1. Except the N₂-Pt system, the Ar-Pt and Ar-Si systems all have a ratio much less than 1, indicating that the gas-gas interaction within the GWIL could be ignored.

Table 1: Mean residence time and gas-gas collision interval in the GWIL of typical systems at the standard conditions.

System	Gas-Solid interaction potential function	h (nm)	$\bar{\tau}$ (ps)	τ_c (ps)
Ar - Pt (1,0,0) plane	Morse potential [24]	0.68	7.60	111
Ar - Si (1,1,1) plane	Lenard-Jones potential [25]	0.93	12.67	91
N ₂ - Pt (1,0,0) plane	Lenard-Jones potential [26]	1.05	42.45	21

3 Validation of the hybrid algorithm

In this section, two benchmark problems, namely 1-D Fourier thermal problem and 1-D Couette shear flow, are simulated to validate the hybrid algorithm. Both the accuracy and efficiency of the hybrid algorithm are compared with that of the pure MD simulations conducted using an open source code "LAMMPS" developed by Sandia National Laboratories.

In both benchmark problems, the solid walls are platinum walls and the gas medium is argon. The Pt-Pt and Ar-Ar interactions are described by the Lenard-Jones (LJ) functions, while a Morse potential function is used for Pt-Ar interaction. All these potential functions are truncated and shifted at the cut-off radius as shown Eq. (3.1) and the associated parameters are listed in Table 2. The nominal thickness of the GWIL is set to be 1.05nm based on the Pt-Ar interaction potential function. Since gas molecules can hardly approach to the surface closer than 0.37nm due to the total repulsive force coming from the entire wall, the effective thickness of the GWIL, h , is 0.68nm for Pt-Ar system. The platinum walls are modeled as atomically smooth flexible thermal walls consisting of 4 layers of FCC structure with (1,1,1) plane facing towards the gas domain. Different constraints are imposed on the bottom layer of solid atoms to control the bulk motions of the wall in the two problems. The rest solid atoms possess thermal vibration and the rescaling thermostat is applied on the atoms per 5,000 MD steps to maintain the wall temperature to be at the prescribed value. The MD time step is 3.15fs. To examine the effect of the thickness of the wall model on the simulation results, a wall model composed of 7 layers of FCC structure is employed to repeat the hybrid DSMC/MD simulation of Fourier thermal problem. Results indicate that the model composed of four layers of FCC structure is sufficient to obtain converged results. Currently the application frequency of the rescaling thermostat is set to be as low as possible provided that it can maintain the mean temperature of the wall model during the rescaling interval with an absolute deviation less than 0.5K. Barisik *et al.* [27] recently pointed out that the thermostat may introduce artificial thermal resistance at the interface between the controlled and non-controlled regions, which may exaggerate the interface thermal resistance if the thermostat is applied adjacent to the liquid-solid interface. In the current gas-solid system, since the rescaling frequency is very low, the induced artificial thermal resistance is expected to be very small. In addition, the gas-solid interface thermal resistance is much larger than that of liquid-solid interface. Hence the influence of the artificial thermal resistance on macro-

Table 2: Molecular interaction parameters.

	$m(\text{g})$	$\sigma(\text{\AA})$	$\varepsilon/k(\text{K})$	$\sigma_0(1/\text{\AA})$	$r_0(\text{\AA})$	$r_c(\text{\AA})$
Pt-Pt	32.4×10^{-23}	2.523	3771.5	—	—	8.83
Ar-Ar	6.63×10^{-23}	3.405	121	—	—	8.83
Pt-Ar	—	—	134.75	1.6	4.6	10.0

scopic flow properties in the gas-solid system would be much less. To justify, another hybrid DSMC/MD simulation of Fourier thermal problem is conducted by employing a wall model composed of 7 layers of FCC structure of which the rescaling thermostat is applied only at the bottom 3 layers of the vibrating solid atoms. Results show that the two sets of simulated macroscopic flow quantities are indistinguishable within the noise level.

$$\phi_{LJ}(r) = 4\epsilon \left[\left(\frac{\sigma}{r} \right)^{12} - \left(\frac{\sigma}{r} \right)^6 \right] - 4\epsilon \left[\left(\frac{\sigma}{r_c} \right)^{12} - \left(\frac{\sigma}{r_c} \right)^6 \right], \quad (3.1a)$$

$$\phi_{Morse}(r) = \epsilon \left[e^{-2\sigma_0(r-r_0)} - 1 \right]^2 - \epsilon \left[e^{-2\sigma_0(r_c-r_0)} - 1 \right]^2. \quad (3.1b)$$

To improve the efficiency, the modified smart wall algorithm described in last section is employed. This technique significantly reduces the memory consumption of MD simulation. In addition, in cases where gas-gas interaction can be ignored in the GWIL, multiple gas molecules are allowed to interact with the wall simultaneously to further reduce the CPU time.

The DSMC simulation domain is divided equally into cells along the transverse direction. Initially 100 simulation particles are generated in each cell. The variable hard sphere (VHS) model is employed for gas-gas collision. The DSMC time step is set as 1/20 of the mean free time, which is about 7ps in the two benchmark problems. The heat flux and stress tensor in the DSMC domain are calculated as follows,

$$q_i = \frac{1}{V} \left\langle \sum^N c_i \left(\frac{1}{2} N_0 m |\mathbf{c}|^2 \right) \right\rangle, \quad (3.2a)$$

$$p_{ij} = \frac{1}{V} \left\langle \sum^N N_0 m c_i c_j \right\rangle, \quad (3.2b)$$

where V is the cell volume, N_0 and N are the number of real gas molecules represented by each DSMC simulation particle and the total number of simulation particles in each cell, c_i is the molecular velocity component in the i direction and $1/2(m|\mathbf{c}|^2)$ is the molecular kinetic energy. In pure MD simulation, the heat flux contains two additional terms relating to potential energy and virial pressure work, and the stress tensor also includes an additional virial term. However, these additional terms are very small (about 0.01% in pressure and 0.1% in heat flux) in the DSMC region. Hence it is reasonable to compare the DSMC results with MD results directly in the DSMC region.

3.1 Fourier thermal problem

The 1-D Fourier thermal problem concerns with the steady heat transfer of gas confined between two parallel stationary walls of different temperatures. A schematic of the problem domain is shown in Fig. 3. The temperatures of the two walls are 400K and 300K, respectively. The separation between the walls is $1\mu\text{m}$. The initial gas temperature is 350K and pressure is 1.1 atm, corresponding to $Kn = 0.06$. The lateral dimensions of the

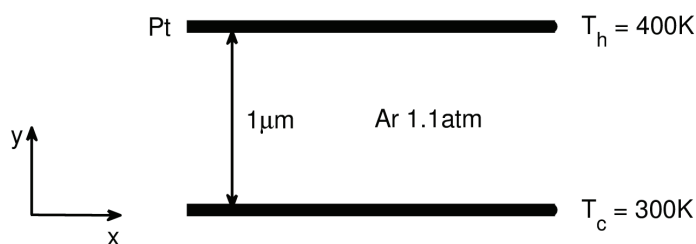


Figure 3: Schematic of the simulation model of the 1-D Fourier thermal problem.

system are set to be $1\mu\text{m}$ by $1\mu\text{m}$. To model the stationary walls, atoms of the bottom layer of the wall model are fixed at the lattice sites without any thermal vibration, which prevents the wall from any translational or rotational motion.

In the pure MD simulation carried out using LAMMPS, the lateral dimensions of the MD system need to be carefully determined. It is found that if the lateral dimensions are too small, a discrepancy between the two tangential temperatures and the normal temperature appears in the bulk region, and an overestimated heat flux results. In general, the lateral dimensions should be at least one mean free path [22]. However, in order to save time, a convergence study is conducted to find the minimum required lateral dimensions for this particular problem. Based on the criterion that the tangential and normal temperatures should be the same in the DSMC region, lateral dimensions with 7.358nm by 8.496nm are selected for this case.

Fig. 4 shows the comparison of the profiles of density, temperature, pressure and heat flux outside the GWIL obtained from the hybrid algorithm and the pure MD simulation respectively. The accuracy of the hybrid algorithm is satisfactory overall. There appears to be a less than 3% discrepancy in the heat flux profile. Based on the convergence study, heat flux decreases with the increased lateral dimensions. Hence the discrepancy is likely caused by the lateral dimensions of the pure MD simulation domain. A larger domain would further reduce the MD heat flux and therefore reduce the discrepancy. In addition, as shown in the density profile in which gas density inside the GWIL calculated based on the effective thickness of the GWIL is also plotted, the hybrid algorithm is also able to capture the gas clustering phenomenon near the wall.

The efficiency of the hybrid algorithm is compared with that of the pure MD simulation by ensuring that the noise levels of macroscopic quantities obtained from the two methods are comparable. Table 3 lists the average noise levels of various quantities and the total sample sizes employed during the steady-state simulation. It is noticed that the heat flux resolved by the hybrid algorithm is slightly noisier than that from the pure MD method, but the pressure and other quantities from the hybrid algorithm are relatively less noisy than that of the pure MD simulation. Both simulations are run on a PC cluster with 16 cores. The hybrid algorithm takes 84 hours to complete while the pure MD simulation takes about 360 hours, so the ratio of the CPU time of two simulations is 0.23. In this benchmark problem, the pure MD model and therefore the number of gas molecules

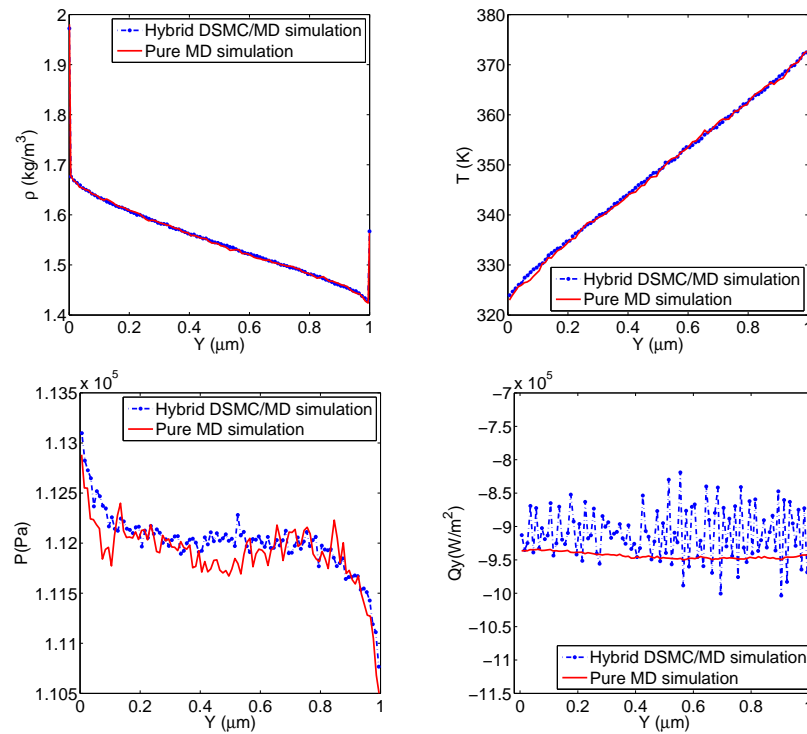


Figure 4: Validation of the hybrid algorithm in 1-D Fourier thermal system: comparison of density, temperature, pressure and heat flux obtained from the hybrid algorithm and the pure MD simulation.

Table 3: The average noise levels of simulated quantities and the corresponding sample sizes employed in Fourier thermal problem.

Noise-to-signal ratio	Density	Temperature	Pressure	Heat flux	Sample size (Million)
Hybrid DMSC/MD simulation	0.1%	0.1%	0.1%	4.5%	3.4
Pure MD simulation	0.2%	0.2%	0.2%	3.0%	1.6

are intentionally set to be small so that results could be obtained within a relatively short period of time. The lateral dimensions of the hybrid model are $1\mu\text{m}$ by $1\mu\text{m}$, much larger than that of the MD model, which are 7.4nm by 8.5nm . If the same size of the model is employed for the pure MD simulation, the computational time would be much greater than 15 days. In both simulations, the most time consuming parts are the simulations of solid-solid interaction and gas-wall interaction since the number of wall atoms is five times of that of gas molecules. The efficiency of the hybrid algorithm demonstrated in this case mostly comes from the use of the smart wall model and the parallel computation of gas-wall interaction in the MD portion. It is expected that the efficiency of the hybrid algorithm would be greater in problems with a large number of gas molecules.

As an application of the developed hybrid algorithm, the 1-D Fourier thermal system is employed to evaluate the performance of the Maxwell model. Being one of the most popular gas-wall interaction models, Maxwell model assumes that a fraction of the incident molecules are reflected diffusely, while the rest undergoes specular reflection. The percentage of the diffuse reflection is quantified by an empirical parameter, the accommodation coefficient, and the velocity distribution of the reflected molecules is given as

$$f_{re} = (1 - \sigma)f_{in} + \sigma f_w(T_w, \vec{v}_w), \quad (3.3)$$

where f_{re} is the velocity distribution function of the reflected molecules, f_{in} is the velocity distribution function of the gas molecules that undergo specular reflection, σ is the accommodation coefficient and $f_w(T_w, \vec{v}_w)$ denotes a half range biased Maxwellian distribution characterized by the wall temperature and velocity T_w and \vec{v}_w as shown in Eq. (3.4),

$$f_w(T_w, \vec{v}_w) = \frac{m^2(v_n - v_{w,n})}{2\pi(kT_w)^2} \exp\left(-\frac{m(\vec{v} - \vec{v}_w)^2}{2kT_w}\right), \quad v_n > v_{w,n}, \quad (3.4)$$

where v_n and $v_{w,n}$ are the normal velocity components of the reflected gas molecule and the wall, respectively. In the 1-D Fourier thermal problem, the relevant accommodation coefficient is the energy accommodation coefficient (EAC), which can be calculated from macroscopic energy fluxes as illustrated in Eq. (3.5),

$$\sigma_e = \frac{e_i - e_r}{e_i - e_w}, \quad (3.5)$$

where e_i and e_r denote the mean total kinetic energy of the incident and reflected gas molecules, and e_w represents the mean kinetic energy of the gas molecules if are fully accommodated with the wall.

The energy accommodation coefficients of the two walls are calculated using the hybrid algorithm based on the incident and reflected velocities at the DSMC/MD interface, and results obtained are 0.399 for the hot wall and 0.412 for the cold wall. Both values are then input into the Maxwell model and used as the boundary model for the pure DSMC simulation. The resolved macroscopic flow fields outside the GWIL together with that obtained from the hybrid algorithm are plotted in Fig. 5. Clearly, the pure DSMC simulation combined with the Maxwell model can predict density, temperature and even heat flux very well outside the GWIL. The relative errors are all smaller than 2%. It is worth noting that the present heat-flux result contradicts with the result of a previous study [21] in which the heat flux calculated from the pure DSMC simulation is distinctly different from that obtained from their hybrid algorithm. A possible reason could be due to the different methods employed for calculating the accommodation coefficients, which lead to different numerical values. For the pressure profile, the pure DSMC simulation predicts a trend that is opposite to that simulated from the hybrid algorithm, revealing certain deficiency in the Maxwell model. This observation further justifies the need for the hybrid algorithm particularly for applications in which pressure is important.

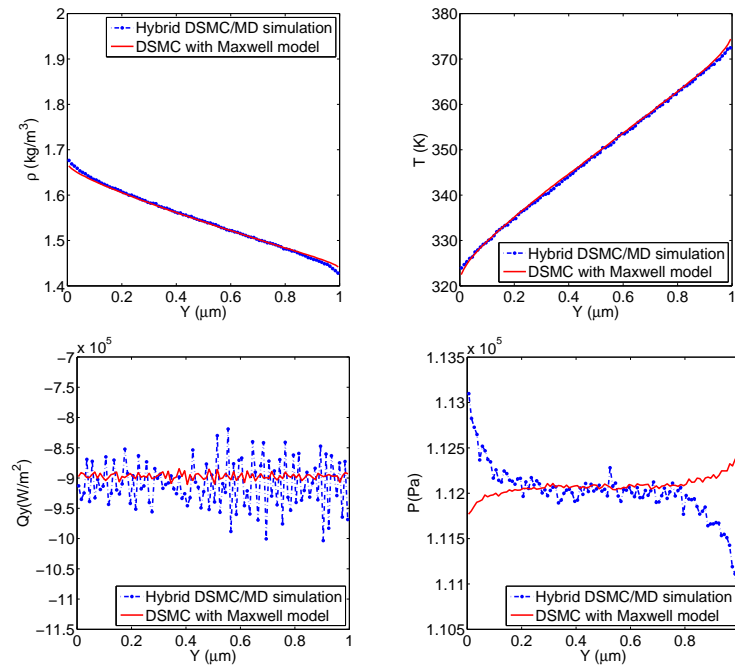


Figure 5: Comparison of macroscopic quantities obtained from the hybrid algorithm and the pure DSMC method combined with Maxwell gas-wall interaction model.

3.2 Couette shear flow problem

As the second validation case, a 1-D Couette shear flow induced by two isothermal parallel walls moving along opposite directions is simulated. The system model and parameters are shown in Fig. 6. The two walls, which are $1\mu\text{m}$ apart and held at 300K, move at 106m/s in opposite directions along the x axis. The initial gas temperature is set to be 300K and the pressure is 96.5kPa, leading to a Knudsen number of 0.057. Due to anti-symmetry, only the lower half of the domain is simulated and the anti-symmetric boundary condition is employed at the center line.

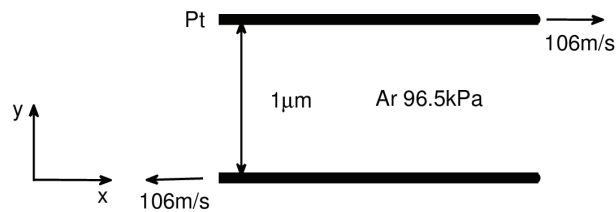


Figure 6: Schematic of the 1-D Couette shear flow system.

Similar to the case of Fourier thermal problem, the lateral dimensions of the system are $1\mu\text{m}$ by $1\mu\text{m}$ and the DSMC domain is divided into 50 equal cells along the normal

direction of the wall. To ensure that the wall model moves at 106m/s along the negative x direction, the velocities of its bottom layer of solid atoms are set to be -106m/s . A convergence study is also conducted to determine the suitable lateral dimensions of the system in the pure MD simulation. Results show that macroscopic properties are not sensitive to the lateral dimensions, and 4.906nm by 5.664nm are sufficient for accurate MD simulation in this case.

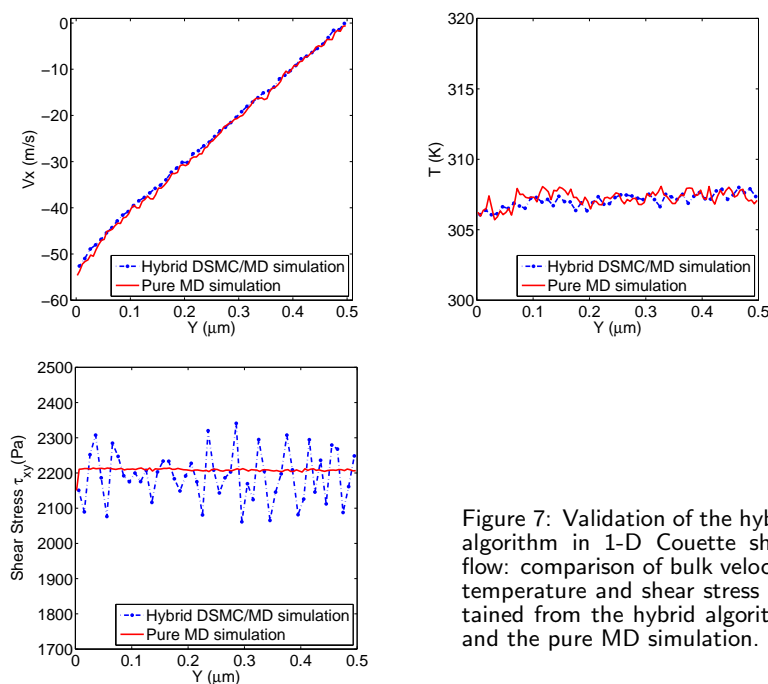


Figure 7: Validation of the hybrid algorithm in 1-D Couette shear flow: comparison of bulk velocity, temperature and shear stress obtained from the hybrid algorithm and the pure MD simulation.

Fig. 7 shows the comparison of the tangential bulk velocity, temperature and shear stress profiles obtained from the hybrid algorithm and the pure MD method. Again, the agreement is very good. The 7K friction induced temperature increment, although small, is well captured by the hybrid algorithm. To obtain the results above, the hybrid algorithm takes 36 hours on 8 cores, while the pure MD simulation needs 240 hours by using the same amount of cores. The CPU time ratio is thus 0.15. The noise levels of the results and sample sizes employed are listed in Table 4.

Table 4: The average noise levels of simulated quantities and the corresponding sample sizes for Couette shear flow problem.

Noise-to-signal ratio	Bulk velocity	Temperature	Shear stress	Sample size (Million)
Hybrid DMSC/MD simulation	1.6%	0.2%	3.6%	1.1
Pure MD simulation	3.5%	0.4%	1.7%	0.9

4 Application of the hybrid algorithm in the prediction of thermal transpiration coefficient

Thermal transpiration is a non-continuum phenomenon induced by the temperature gradient in a rarefied gas. Fig. 8 illustrates a typical thermal transpiration system in which a narrow channel is connected to two large gas chambers. Gas temperatures inside the two chambers are maintained at different levels, and as such, a temperature gradient along the channel length is established. This temperature gradient together with the gas rarefaction effect promotes gas to flow from one chamber to the other chamber near the channel wall, which in turn creates a pressure gradient at the steady state. This can be utilized in various applications, for example, the Knudsen pump [19,28].

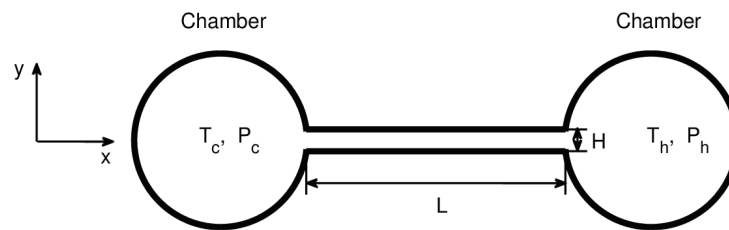


Figure 8: System model of thermal transpiration problem.

The pressure gradient can be quantified by the thermal transpiration coefficient γ defined as follows,

$$\left(\frac{P_h}{P_c}\right) = \left(\frac{T_h}{T_c}\right)^\gamma, \quad (4.1)$$

where T_h , T_c , P_h and P_c are the temperature and pressure in the two chambers. Several studies [29,30] have investigated the influence of the empirical gas-wall interaction models on the thermal transpiration coefficient. In the free-molecule regime, it was found that the Maxwell model yielded a constant γ of 0.5 independent of the accommodation coefficients, while the Cercignani-Lampis (CL) model predicted a value of γ which deviates significantly from 0.5 and varies with the tangential energy accommodation coefficient.

To evaluate the accuracy of the thermal transpiration coefficients predicted by the two popular gas-wall interaction models, the developed hybrid algorithm is employed to study the transpiration system. Fig. 9 shows the simulation model, which is a simplified version of the original system. The two chambers are replaced by two closed vertical walls at which fully diffuse boundary conditions are prescribed to ensure that gas molecules reflected from those walls are from equilibrium reservoirs with the prescribed temperatures. Due to symmetry, only the lower half of the channel is simulated. Specular boundary condition is applied at the symmetric line. The system is again composed of atomically smooth platinum wall and argon gas. System parameters are set as follows: $L=10\mu\text{m}$, $H=1\mu\text{m}$, $T_c=275\text{K}$, $T_h=325\text{K}$. In the simulation, the linear temperature profile of the wall is approximated by piecewise constant profile. The platinum wall is divided

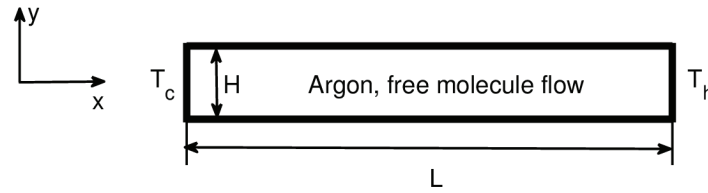


Figure 9: Simulation model of the thermal transpiration problem illustrated in Fig. 8.

evenly into 50 sections, each of which is assumed to have a uniform temperature set to be the wall temperature at its center. Rescaling thermostat is used to maintain its temperature at the prescribed value and periodic boundary condition is applied at its lateral directions. To examine the discretization error, a simulation with 100 sections is also conducted. The maximum differences in temperature, density and pressure profiles obtained from the two simulations are only 0.2%. The implementation of the MD portion follows that in the modeling of Fourier thermal problem. The DSMC gas domain is divided into 50 equal cells along x direction, each contains 100 simulation particles initially. The initial gas density and temperature are set to be 0.1545kg/m^3 and 300K , respectively. Collision procedure in the DSMC is turned off in order to simulate free molecular flow. The coupling between the DSMC and the MD simulation is conducted section-wise. Simulation particles crossing the DSMC/MD interface are assigned into different wall sections based on their locations, providing the incident velocity distribution for the corresponding MD simulation domain.

Fig. 10 presents the profiles of various macroscopic properties along the channel length. The thermal transpiration coefficient γ is estimated following a method proposed in [30], that is, from Eq. (4.2),

$$\rho(x)[T(x)]^{1-\gamma} = \text{const.} \quad (4.2)$$

When the channel is narrow and long, it is expected that γ obtained from the present model is fairly closed to that in the original system. For the current Ar-Pt system in the free-molecule regime, γ calculated from Eq. (4.2) based on the density and temperature profiles simulated from the hybrid algorithm is about 0.14.

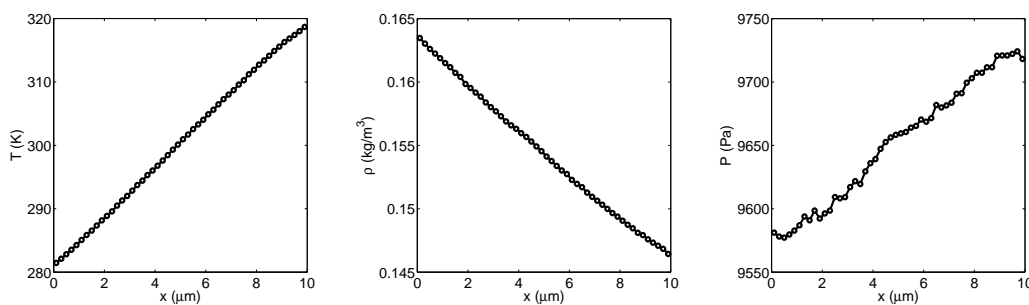


Figure 10: The profiles of macroscopic properties along the axial direction of the channel.

To facilitate the comparison with the values obtained from CL model, energy accommodation coefficients are calculated. Due to the small temperature difference between the gas and the wall in this case, the EACs extracted from the hybrid DSMC/MD simulation are subject to a large statistical noise. In addition, the EACs vary along the length of the channel. The EAC for the normal velocity component varies between 0.1~0.4 near the cold end and 0.5~0.9 near the hot end, while the EAC for the tangential velocity component is between 0.2~0.35 near both ends. The CL model requires the energy accommodation coefficients of both the normal and tangential components, that is, α_n and α_t , as shown as follows:

$$P(\vec{c}' \rightarrow \vec{c}) = \left(\frac{m}{kT_w} \right)^2 \frac{c_n}{2\pi\alpha_n\alpha_t} \exp \left\{ -\frac{m}{2kT_w} \frac{[\vec{c}'_t - \sqrt{1-\alpha_t}\vec{c}'_t]^2}{\alpha_t} \right\} \\ \times \exp \left\{ -\frac{m}{2kT_w} \frac{c_n^2 + (1-\alpha_n)c_n'^2}{\alpha_n} \right\} I_0 \left(\frac{m}{kT_w} \frac{\sqrt{1-\alpha_n}c'_n c_n}{\alpha_n} \right), \quad (4.3)$$

where $P(\vec{c}' \rightarrow \vec{c})$ denotes the probability of a molecule with the incident velocity \vec{c}' being reflected from the wall with the velocity \vec{c} , the subscript w represents the wall, n and t are the normal and tangential velocity components. I_0 denotes the zeroth-order modified Bessel function of the first kind.

Due to the relatively large variation in the calculated EACs, thermal transpiration coefficients are calculated at various different EACs and results are plotted in Fig. 11. It is evident that the thermal transpiration coefficient predicted from Cercignani-Lampis model is almost independent with the EAC associated with the normal velocity component, but varies quite significantly with the EAC associated with the tangential velocity component. Within the range of the accommodation coefficients calculated from the hybrid simulation, the transpiration coefficient obtained from the CL model varies between

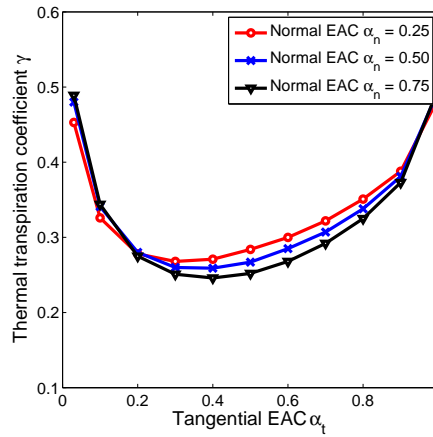


Figure 11: Thermal transpiration coefficient simulated from the DSMC simulation combined with CL model.

0.25-0.3, all are higher than the 0.14 predicted from the hybrid algorithm. Nevertheless, compared to the value obtained from the Maxwell model, the CL model produces a much more accurate thermal transpiration coefficient, which is consistent with the conclusions of the previous studies [29,30].

5 Conclusions

An efficient hybrid DSMC/MD scheme for the simulation of micro gas flows is developed. In this scheme, MD simulation is employed to obtain accurate boundary conditions for the DSMC simulation, while the DSMC simulation provides the incident gas molecule information to the MD simulation. The coupling between the two methods is realized by matching the velocity distribution function at the DSMC/MD interface, and therefore the mass, momentum and energy fluxes are conserved across the interface. The efficiency of the hybrid algorithm comes from three aspects: (1) the MD is applied only within the gas-wall interaction layer and the majority of the gas domain is simulated by the DSMC, (2) a smart-wall model [22] is employed which greatly reduces the memory consumption of the MD simulation, and (3) gas-gas interaction is ignored within the gas-wall interaction layer if gas is rarefied within the layer.

The developed algorithm is employed to evaluate the performance of Maxwell gas-wall interaction model on the simulation of the 1-D Fourier thermal flow. It is found that while the temperature, density and heat flux profiles outside the gas-wall interaction layer predicted quite well by the DSMC combined with Maxwell model, the trend of the pressure profile is opposite to that simulated from the hybrid algorithm, indicating the deficiency of the Maxwell model. The hybrid algorithm is also employed to calculate the thermal transpiration coefficient in the free-molecule regime. The result is compared to that obtained from Maxwell and CL models. A closer agreement between the results from the hybrid algorithm and the CL model is obtained.

Acknowledgments

This work is supported in part by Award No. SA-C0040/UK-C0016, made by King Abdullah University of Science and Technology, and in part by Hong Kong Research Grants Council under Competitive Earmarked Research Grant 621408.

References

- [1] R. Leung, H. Cheung, H. Gang and W. Ye, A Monte Carlo Simulation approach for the modeling of free-molecule squeeze-film damping of flexible microresonators, *Microfluid. Nanofluid.*, 9(2010), 809-818.
- [2] T. Ohwada, Y. Sone and K. Aoki, Numerical analysis of the Poiseuille and thermal transpiration flows between two parallel plates on the basis of the Boltzmann equation for hard-sphere molecules, *Phys. Fluids A*, 1(1989), 2042.

- [3] T. Ohwada, Y. Sone and K. Aoki, Numerical analysis of the shear and thermal creep flows of a rarefied gas over a plane wall on the basis of the linearized Boltzmann equation for hard-sphere molecules, *Phys. Fluids A*, 1(1989), 1588.
- [4] Y. Sone, T. Ohwada and K. Aoki, Temperature jump and Knudsen layer in a rarefied gas over a plane wall: Numerical analysis of the linearized Boltzmann equation for hard-sphere molecules, *Phys. Fluids A*, 1(1989), 363.
- [5] K. Xu and J. C. Huang, A unified gas-kinetic scheme for continuum and rarefied flows, *J. Comput. Phys.*, 229(2010), 7747-7764.
- [6] K. Xu and J. C. Huang, An improved unified gas-kinetic scheme and the study of shock structures, *J. Inst. Math. Its Appl.*, 76(2011), 698-711.
- [7] D. C. Rapaport, *The Art of Molecular Dynamics Simulation*. Cambridge Univ Pr, 2004.
- [8] G. A. Bird, *Molecular gas dynamics and the direct simulation of gas flows*, 1994.
- [9] J. C. Maxwell, On stresses in rarified gases arising from inequalities of temperature, *Philos. Trans. R. Soc. London*, 170(1879), 231-256.
- [10] C. Cercignani and M. Lampis, Kinetic models for gas-surface interactions, *Transp. Theory Stat. Phys.*, 1(1971), 101-114.
- [11] E. B. Arkilic, K. S. Breuer and M. A. Schmidt, Mass flow and tangential momentum accommodation in silicon micromachined channels, *J. Fluid Mech.*, 437(2001), 29-43.
- [12] T. Ewart, P. Perrier, I. Graur and J. G. Molans, Tangential momentum accommodation in microtube, *Microfluid. Nanofluid.*, 3(2007), 689-695.
- [13] A. Agrawal and S. Prabhu, Survey on measurement of tangential momentum accommodation coefficient, *J. Vac. Sci. Technol., A*, 26(2008), 634.
- [14] D. Bruno, M. Cacciatore, S. Longo and M. Rutigliano, Gas-surface scattering models for particle fluid dynamics: a comparison between analytical approximate models and molecular dynamics calculations, *Chem. Phys. Lett.*, 320(2000), 245-254.
- [15] K. Yamamoto, H. Takeuchi and T. Hyakutake, Characteristics of reflected gas molecules at a solid surface, *Phys. Fluids*, 18(2006), 046103.
- [16] K. Yamamoto, H. Takeuchi and T. Hyakutake, Scattering properties and scattering kernel based on the molecular dynamics analysis of gas-wall interaction, *Phys. Fluids*, 19(2007), 087102.
- [17] N. D. Masters, W. Ye and W. P. King, The impact of subcontinuum gas conduction on topography measurement sensitivity using heated atomic force microscope cantilevers, *Phys. Fluids*, 17(2005).
- [18] T. Zhu and W. Ye, Origin of Knudsen forces on heated microbeams, *Phys. Rev. E*, 82(2010), 036308.
- [19] N. K. Gupta, N. D. Masters, W. Ye and Y. B. Gianchandani, Gas flow in nano-channels: Thermal transpiration models with application to a silicon micromachined Knudsen pump, in *Transducers '07, Int. Conf. Solid-State Sens., Actuators Microsyst.*, 2007, 2329-2332.
- [20] S. Nedeaa, A. Frijns, A. van Steenhoven, A. Markvoort and P. Hilbers, Hybrid method coupling molecular dynamics and Monte Carlo simulations to study the properties of gases in microchannels and nanochannels, *Phys. Rev. E*, 72(2005), 016705.
- [21] K. Gu, C. B. Watkins and J. Koplik, Atomistic hybrid DSMC/NEMD method for nonequilibrium multiscale simulations, *J. Comput. Phys.*, 229(2010), 1381-1400.
- [22] M. Barisik, B. Kim and A. Beskok, Smart wall model for molecular dynamics simulations of nanoscale gas flows, *Commun. Comput. Phys.*, 7(2010), 977-993.
- [23] M. Barisik and A. Beskok, Equilibrium molecular dynamics studies on nanoscale-confined fluids, *Microfluid. Nanofluid.*, 11(2011), 269-282.

- [24] K. Yamamoto, Slip flow over a smooth platinum surface, *JSME Int. J., Ser. B*, 45(2002), 788-795.
- [25] S. Satake, N. Inoue, T. Kunugi, M. Shibahara and H. Kasahara, Large-scale molecular dynamics simulation for two Ar clusters impact on 4H-SiC, *Nucl. Instrum. Methods Phys. Res., Sect. B*, 257(2007), 639-644.
- [26] P. Zeppenfeld, R. David, C. Ramseyer, P. N. M. Hoang and C. Girardet, Adsorption and structure of N₂ on Pt(111), *Surf. Sci.*, 444(2000), 163-179.
- [27] M. Barisik and A. Beskok, Boundary treatment effects on molecular dynamics simulations of interface thermal resistance, *J. Comput. Phys.*, 231(2012), 7881-7892.
- [28] N. K. Gupta and Y. B. Gianchandani, A knudsen pump using nanoporous zeolite for atmospheric pressure operation, in *Micro Electro Mech. Syst., IEEE Int. Conf.*, 21st, 2008, 38-41.
- [29] F. Sharipov, Application of the Cercignani-Lampis scattering kernel to calculations of rarefied gas flows. III. Poiseuille flow and thermal creep through a long tube, *European Journal of Mechanics, B: Fluids*, 22(2003), 145-154.
- [30] O. Sazhin, A. Kulev, S. Borisov and S. Gimelshein, Numerical analysis of gas-surface scattering effect on thermal transpiration in the free molecular regime, *Vacuum*, 82(2007), 20-29.